Journal of Bone and Mineral Research, 2025, **00**, 1–10
https://doi.org/10.1093/jbmr/zjaf082
Advance access publication: June 11, 2025
Research Article

Improvements in hearing loss with bone-targeted enzyme replacement therapy are associated with corrected hypomineralization and osteocyte properties of auditory ossicles in Enpp1-deficient mice

Ana Ocokoljic[1], Shivani Srivastava[2], Simon von Kroge[1,3], Paul R. Stabach[2], Björn Busse[3], Keith Weise[2], Ralf Oheim[3], Tim Rolvien[1,*], Demetrios T. Braddock[2,*]

[1]Division of Orthopaedics, Department of Trauma and Orthopedic Surgery, University Medical Center Hamburg-Eppendorf, 20246 Hamburg, Germany
[2]Department of Pathology, Yale University School of Medicine, New Haven, CT 06510, United States
[3]Institute of Osteology and Biomechanics, University Medical Center Hamburg-Eppendorf, 20246 Hamburg, Germany
*Corresponding authors: Tim Rolvien, Department of Trauma and Orthopedic Surgery, University Medical Center Hamburg-Eppendorf, Martinistr. 52, 20246 Hamburg, Germany (t.rolvien@uke.de); Demetrios T. Braddock, Department of Pathology, Yale University School of Medicine, New Haven, CT 06510, United States (demetrios.braddock@yale.edu).

Abstract

Hearing loss is common in conditions caused by ectonucleotide pyrophosphatase/phosphodiesterase 1 (ENPP1) deficiency, such as generalized arterial calcification of infancy and autosomal recessive hypophosphatemic rickets type 2. Mechanistically, it is hypothesized that poor mineralization of the auditory ossicles leads to impaired sound transmission in the middle ear. Here we investigated whether enzyme replacement therapy (ERT) improves hearing loss in an Enpp1-deficient mouse model and whether this is associated with corrected bone properties in the ossicles. For this purpose, male *Enpp1*$^{asj/asj}$ mice were subjected to either a soluble or bone-targeted ERT of ENPP1-Fc. Hearing function and bone properties of the malleus, the first bone of the ossicular chain, were evaluated and compared to untreated *Enpp1*$^{asj/asj}$ and WT mice at the age of 17 wk. In untreated Enpp1-deficient mice, we found elevated hearing thresholds at stimulus frequencies of 8, 16, and 32 kHz, suggesting a generalized impairment of hearing. The hearing deficits observed in *Enpp1*$^{asj/asj}$ mice were partially or fully corrected by both soluble and bone-targeted ERT, as evidenced by the restoration of auditory brainstem response thresholds, with dose dependence and generally stronger effect of bone-targeted ERT. This was not only associated with corrected blood plasma markers of mineral metabolism but also improved matrix mineralization and restored osteocyte properties in the malleus. In addition, for the first time in mice, we were able to demonstrate the occurrence of mineralized osteocyte lacunae in *Enpp1*$^{asj/asj}$ mice, a phenomenon that was corrected by bone-targeted but not soluble ERT, underscoring the need for targeted delivery for effective treatment. In contrast to osteocyte lacunar mineralization in humans (ie, micropetrosis), the intra-lacunar mineral was overall less mineralized than the adjacent bone. In conclusion, our results point toward the potential benefit of correcting ossicular mineralization to prevent hearing loss in ENPP1 deficiency.

Keywords: Enpp1, mineralization, hearing loss, osteocyte lacunae, animal model

Lay Summary

Hearing loss is common in conditions caused by ectonucleotide pyrophosphatase/phosphodiesterase 1 (ENPP1) deficiency, likely due to poor mineralization of the ossicles. This study tested whether enzyme replacement therapy (ERT) could improve hearing in Enpp1-deficient mice. Both soluble and bone-targeted ERT improved hearing, with bone-targeted ERT showing stronger effects. This improvement was associated with the restoration of ossicular bone properties and the correction of abnormal osteocyte lacunar mineralization. Taken together, these findings suggest that targeting bone mineralization in the middle ear may help prevent hearing loss in ENPP1 deficiency.

Introduction

Ectonucleotide pyrophosphatase/phosphodiesterase 1 (ENPP1) encodes an enzyme essential for skeletal mineralization processes. This enzyme plays a critical role in the regulation of mineralization by catalyzing the hydrolysis of adenosine triphosphate (ATP) to adenosine monophosphate (AMP) and pyrophosphate (PP_i).[1] Variants in the *ENPP1* gene cause several disorders, including generalized arterial calcification of infancy (GACI), autosomal recessive hypophosphatemic rickets type 2 (ARHR2), early-onset osteoporosis (EOOP), and ossification of the spinal ligaments (OPLL and DISH).[2–8]

In addition to these conditions, variants in *ENPP1* have been associated with hearing loss in patients,[2–4] a phenotype recapitulated in Enpp1-deficient mice.[9] Previous research has linked conductive hearing loss to mineralization defects in auditory ossicles in other genetic conditions of impaired bone mineralization.[10] Despite the major burden associated with *ENPP1* variants for patients, therapeutic options remain

Received: November 22, 2024. **Revised:** June 3, 2025. **Accepted:** June 7, 2025
© The Author(s) 2025. Published by Oxford University Press on behalf of the American Society for Bone and Mineral Research. All rights reserved. For commercial re-use, please contact reprints@oup.com for reprints and translation rights for reprints. All other permissions can be obtained through our RightsLink service via the Permissions link on the article page on our site—for further information please contact journals.permissions@oup.com.

Downloaded from https://academic.oup.com/jbmr/advance-article/doi/10.1093/jbmr/zjaf082/8160135 by ASBMR Member Access user on 04 August 2025

underexplored. For example, oral phosphate supplementation has been investigated but did not provide sufficient improvements regarding the skeletal abnormalities of the patients and was further associated with nephrocalcinosis.[2] Enzyme replacement therapy (ERT) using a soluble recombinant Enpp1-Fc protein has shown improvements in bone mass and suppression of nephrocalcinosis in Enpp1-deficient mice.[2] However, it remains unclear whether ERT can effectively prevent the hearing-related abnormalities. Additionally, there is still considerable uncertainty regarding the optimal formulations and dosages for ERT.

Therefore, we aimed to investigate the potential of newly developed ERT formulations to ameliorate functional hearing impairments and to correct both structural and cellular alterations of the auditory ossicles in the *Enpp1*$^{asj/asj}$ mouse model. Specifically, we examined the effects of a soluble (ERT 1118) and bone-targeted (ERT 2000) form of ENPP1, aiming to decipher how these treatments differentially influence hearing capacity and middle ear bone matrix properties.

Materials and methods

Animals

Animal care and maintenance were conducted at the Yale University Animal Resource Center, New Haven, CT, USA. All experimental procedures were approved by the Animal Care and Use Committee of Yale University and adhered to the U.S. National Institutes of Health guidelines for the care and use of laboratory animals. We used male *Enpp1*$^{asj/asj}$ mice generated as described previously[11] and WT littermates. *Enpp1*$^{asj/asj}$ mice possess a missense mutation in *Enpp1* (Val246Asp).[12,13] The mice had ad libitum access to food and water throughout the study. The colony was maintained under specific pathogen-free conditions to ensure a controlled environment.

ERT formulations

The design and characterization of Enpp1-Fc clone 1118 has been previously described.[14] Soluble 1118 was targeted to the bone via a 6 aspartic-acid C-terminal tag (clone 2000) introduced via site-directed mutagenesis using the QuikChange XL Site-Directed Mutagenesis Kit (Agilent Technologies Catalog #200516), following manufacturer's protocols. The sense and anti-sense oligos were 5′ CTGTCTCCGGGTAAAGATGATGATGATGATGATGACGACTGAGTGCTAGCTGGCCAG 3′ and 5′ GCCAGCTAGCACTCAGTCGTCATCATCATCATCATCATCTTTACCCGGAGACAGGGAG 3′. Plasmids were sequence verified correctly through the Yale Keck DNA Sequencing core facility. Both proteins were purified as previously described.[13] Further, the ERT 1118 and ERT 2000 were formulated in a vehicle consisting of Bio-Rad Laboratories 10× TBS (stock number 1706435) diluted to 1× with endotoxin-free water and supplemented with 20 μM $CaCl_2$ and 20 μM $ZnCl_2$.

Application of ERT

After weaning, *Enpp1*$^{asj/asj}$ mice were randomly assigned to 1 of 6 groups, receiving weekly subcutaneous injections of either vehicle, soluble ENPP1 (ERT 1118) at 1, 2, or 4 mg/kg body weight, or bone-targeted ENPP1 (ERT 2000) at 0.5 or 1 mg/kg body weight (Figure 1A). Unaffected WT siblings were used as controls and received weekly subcutaneous injections of the vehicle. All animals received weekly i.p. injections of anti-murine CD4 to suppress autoimmune rejection of the human biologics, dosed 24 h prior to treatment with ENPP1 (75 μL prior to the first ENPP1 dose and 50 μL thereafter; GK 1.5, Life Technologies Corporation; 1 mg/mL of solution; cat #16-0041-95). At 17 wk of age, blood samples were taken, the mice were tested for hearing function, sacrificed, and prepared for further analysis.

Blood plasma measurements

Blood samples were separated by centrifuging at 1000 × *g* for 10 min at 4 °C. Alkaline phosphatase levels in the plasma were quantified using a colorimetric assay kit from Abcam Corporation (catalog number: ab83369). ELISA kits for measuring mouse PTH1-84 and FGF-23 were sourced from Quidel Corporation (catalog numbers: 60-2305 and 60-6800) and used as per the manufacturer's instructions. Plasma phosphate and calcium levels were assessed by the George M. O'Brien Kidney Center Animal Physiology and Phenotyping Core at Yale.

Hearing tests

Auditory brainstem response (ABR) testing and data collection were performed by TurnerScientific LLC using a trained objective ABR reviewer, who was blinded to the treatment conditions. The reviewer employed a compact auditory electro-diagnostic system to conduct the testing. The acoustic stimulus presentation, ABR acquisition, equipment control, and data management were coordinated using Tucker Davis Technologies (TDT) Hardware consisting of an RV6 processing unit, Medusa4Z headstage preamplifier, and BioSigRZ and SiggenRZ Software. Calibration of the acoustic signals was conducted at the beginning of each day of testing with Turner Scientific's Sensory Sentinel mobile environmental monitoring and acoustic measurement system (https://www.turnerscientific.com/products-1), consisting of a 1/4" microphone with a relatively flat response through the mouse hearing range, an acoustic calibrator, a Precision Data Acquisition Unit (192 kHz sampling rate, 24 bit, IEPE power), and custom Sensory Sentinel acoustics processing software. Acoustic calibration measurements were collected using an ear canal model such that the intensity was measured approximately 1 cm from the tip of the speaker output, using a semi-closed coupler to approximate the fit of the speaker output into the canal, to simulate the pressure present at the animal's tympanic membrane. Sound stimuli were calibrated in dB SPL (unweighted peak sound pressure level, re: 20 μPa).

Mice were anesthetized with ketamine/xylazine. ABRs were recorded unilaterally using 3 stainless steel needle electrodes placed sub-dermally over the vertex (noninverting electrode) and the ipsilateral (speaker side) mastoid. Ground electrodes were placed either at the opposite mastoid or on the back. Acoustic stimuli were generated by the TDT system and presented to one ear via a high-frequency transducer (TDT MF1, closed field) directed into the canal as close to the canal tissue as possible without sealing against tissue or blocking the canal. The sound stimuli consisted of tone bursts with rise-fall times of 0.1 ms and plateaus of 1.5 ms at frequencies of 8, 16, and 32 kHz. The biological signals were amplified, averaged, stored, and displayed on the computer screen. Sound intensities were presented at descending intensity steps from 80 to 5 dB in 5 dB steps. All electronic data were stored for off-line, blinded analysis.

Downloaded from https://academic.oup.com/jbmr/advance-article/doi/10.1093/jbmr/zjaf082/8160135 by ASBMR Member Access user on 04 August 2025

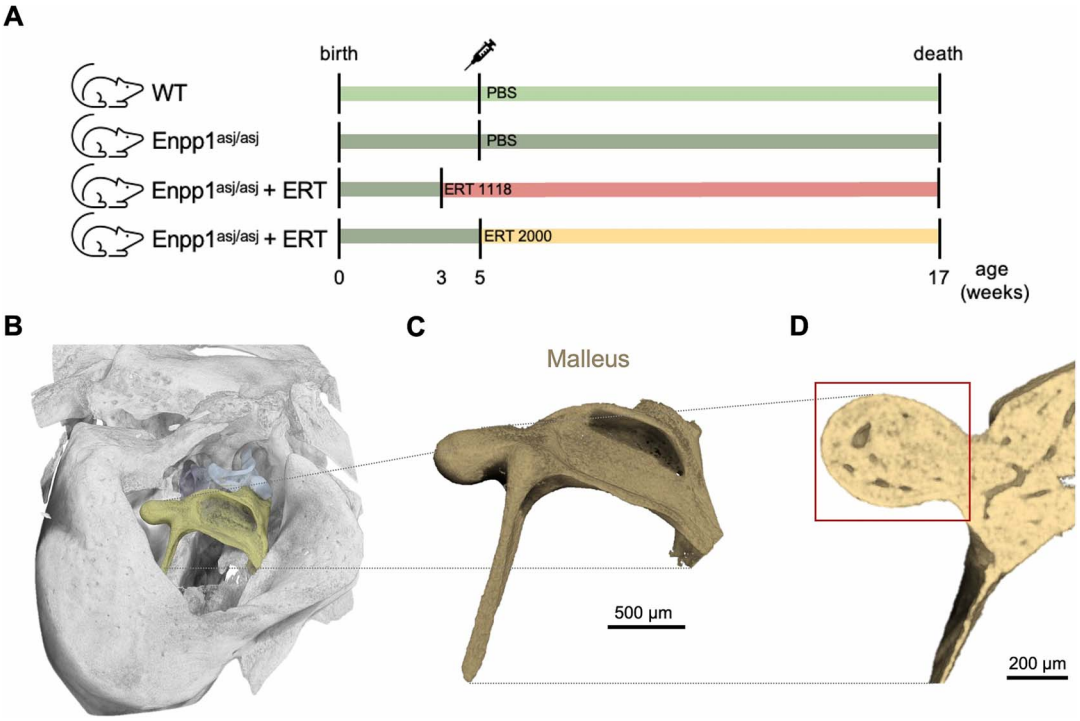

Figure 1. Study design and definition of the region of interest for analysis of the auditory ossicles (malleus). (A) Schematic representation of the enzyme replacement therapy (ERT) regimen. PBS, phosphate-buffered saline. (B) Representative μCT scan of the ossicles within the temporal bone. (C) Three-dimensional and (D) cross-section view of the malleus showing the defined region of interest (malleal processus brevis).

Determination of ABR thresholds was conducted by an ABR reviewer, who was blinded to the treatment conditions. A non-repeating, random number was assigned to each ABR wave file to be analyzed such that the reviewer could determine the threshold without knowing the subject's treatment condition. The blinded reviewer then determined the lowest intensity at which any discernible waveform could be identified. After all thresholds were determined, animal ID numbers were unmasked and threshold shifts (the change in hearing threshold from baseline to terminal ABR) at each test frequency were computed. The blinded ABR threshold determinations at Turner Scientific have previously been shown to be highly reliable, with duplicate thresholds correlating at $r = +0.97$ (Pearson's r).

Sample preparation

The preparation and isolation of middle ears and auditory ossicles were conducted using a stereomicroscope as reported previously.[15] To standardize the analyses, the malleus of the animals was extracted, fixed in 3.7% formaldehyde, subjected to a graded ethanol dehydration series, and embedded undecalcified in methyl methacrylate. Next, polishing of the embedded specimen was performed on an EXAKT 400 CS surface grinding machine (EXAKT). The process began with 1200 grit silicon carbide wet sandpaper (Allied High Tech Products Inc.) adjusting the grinding time for each specimen to achieve the ideal cross-section. Upon achieving the optimal cross-section visually, further polishing was conducted for four minutes using 4000-grit silicon carbide wet sandpaper.[15]

Quantitative backscattered electron imaging

To assess the mineralization of the embedded malleus, its BMD distribution (BMDD) was assessed using quantitative backscattered electron imaging (qBEI). The samples were polished, coated with carbon, and imaged using a scanning electron microscope (LEO 435 VP; LEO Electron Microscopy Ltd.) attached with a backscattered electron detector (type 202; K.E. Developments Ltd.; 20 kV, 680 pA, 20 mm working distance) as previously described.[16,17] Calibration of brightness and contrast in the qBEI images was performed using carbon (gray value: 5.0 ± 0.5) and aluminum standards (gray value: 222.4 ± 0.5). To standardize our assessment across specimens, all analyses were conducted on a standardized region of the malleus (malleal processus) (Figure 1B-D). For the BMDD analysis, the magnification was 100× at a resolution of 1.1 μm/pixel. The mean calcium content (CaMean, wt%), the peak calcium content (CaPeak, wt%), and the mineralization heterogeneity (CaWidth, wt%) were determined using a custom MATLAB-based script quantifying the acquired gray-value-based images (MathWorks, Inc.). For the osteocyte analysis, independent sets of images were acquired with a magnification of 400× and a resolution of 0.096 μm/pixel. The acquired images were further analyzed with respect to osteocyte lacunar parameters, that is, the total number of osteocyte lacunae per bone area (N.Tt.Ot.Lc/B.Ar, 1/mm^2) and the mean osteocyte lacunar area (Ot.Lc.Ar, μm^2). Furthermore, the number of non-mineralized (N.Non.Min.Ot.Lc/B.Ar, 1/mm^2) and mineralized lacunae (N.Min.Ot.Lc/B.Ar, 1/mm^2) were counted manually. For the analysis of intra-lacunar mineralization (CaMean), the images were manually processed to evaluate either the mineral of the corresponding mineralized lacunae or the surrounding bone using the MATLAB routine.

Energy dispersive X-ray absorptiometry

The composition of lacunar mineralization was further characterized by energy dispersive X-ray absorptiometry (EDX). Subsequent to qBEI measurements, samples of untreated (ie,

Downloaded from https://academic.oup.com/jbmr/advance-article/doi/10.1093/jbmr/zjaf082/8160135 by ASBMR Member Access user on 04 August 2025

vehicle-treated) or ERT 1118-treated (1 mg/kg, 2 mg/kg, 4 mg/kg) Enpp1-deficient mice were analyzed using a Crossbeam 340 system assembled with an EDX detector (X-Max 80, Oxford Instruments). The system was operated at a voltage of 30 kV and an acceleration current of 400 pA. To assess the composition and the calcium-to-phosphate ratio of osteocyte lacunae and the surrounding matrix, point measurements were taken within mineralized lacunae and the bone matrix at a 5000× magnification. Per measurements, 1 million counts were taken to get a representative amount of information. Data on lacunar mineralization in WT mice and Enpp1-deficient mice treated with ERT 2000 were not assessed due to the low number of mineralized lacunae in these mice.

Statistical analysis

Statistical analysis was performed using GraphPad Prism (version 10, GraphPad Software). Data are shown as box plots with dots representing individual values and indicating the group size. To test for differences between groups, we first performed a one-way ANOVA, and in case of overall significant differences, then performed Sidak's multiple comparisons tests between WT controls and untreated *Enpp1*$^{asj/asj}$ mice and between WT or untreated *Enpp1*$^{asj/asj}$ mice and all treatment groups. Individual multiple comparisons tests among all different treatment groups were not performed for reasons of clarity. For the additional comparison of CaMean values, ANOVA with Sidak's multiple comparisons tests was performed to test for differences between genotypes (WT vs *Enpp1*$^{asj/asj}$) and anatomic locations (malleus vs femur). All statistical tests were 2-sided, and a significance threshold of 0.05 was chosen.

Results

Most plasma biomarkers of mineral metabolism are corrected by bone-targeted ERT

Analyses of blood samples showed that the bone-targeted ERT successfully normalized alkaline phosphatase levels to physiological levels (Figure 2A). However, while soluble ERT effectively normalized phosphate levels, bone-targeted ERT did not achieve this correction (Figure 2B). Notably, calcium levels remained stable in *Enpp1*$^{asj/asj}$ mice, showing no significant changes with either form of ERT (Figure 2C). Furthermore, neither bone-targeted nor soluble ERT corrected FGF23 levels, and while soluble ERT elevated the reduced PPi in *Enpp1*$^{asj/asj}$ mice to supraphysiologic levels, bone-targeted ERT at the higher dose normalized plasma PPi to WT levels (Figure 2D and E). Interestingly, bone-targeted ERT resulted in suppressed PTH below WT levels compared to soluble ERT (Figure 2F).

Hearing loss is prevented by bone-targeted ERT (2000)

Based on the reported hearing loss in patients with *ENPP1* variants, the auditory phenotype of *Enpp1*$^{asj/asj}$ mice and their WT littermates was assessed using ABR, which reflects the cumulative electrical activity of the auditory nerve and central auditory pathways. We found that untreated Enpp1-deficient mice exhibited elevated hearing thresholds at stimulus frequencies of 8, 16, and 32 kHz, suggesting a generalized impairment of hearing (Figure 3A-C). At 8 kHz, administration of the soluble form of the enzyme at a low dose (1 mg) did not restore hearing function. However, higher doses normalized hearing performance. Similarly, a dose of 0.5 or 1 mg of the bone-targeted form effectively normalized the hearing threshold (Figure 3A). At 16 kHz, the hearing threshold was normalized by administering the soluble form at higher doses (2 and 4 mg) and partly corrected the bone-targeted form at 1 mg (Figure 3B). In the high-frequency hearing range (ie, at 32 kHz), the soluble form did not consistently normalize hearing thresholds (Figure 3C). However, the higher dose of the bone-targeted form (1 mg) was able to fully normalize auditory function, suggesting that bone-targeted ERT restores hearing in the low and high frequency range.

Bone-targeted ERT prevents mineralization defects

Mineralization of the auditory ossicles is a critical factor in conductive hearing performance.[10] Therefore, we analyzed the mineralization characteristics of the malleus in WT, untreated Enpp1-deficient, and treated Enpp1-deficient mice using qBEI (Figure 4A). Untreated Enpp1-deficient mice showed a trend toward lower mean matrix mineralization (CaMean) and significantly lower peak matrix mineralization than WT controls (Figure 4B and C). Interestingly, the administration of the soluble ERT (1118) partially rescued the mineralization defect, while the bone-targeted ERT resulted in a full correction. The mineralization heterogeneity (CaWidth), which indicates skeletal remodeling activity, showed no differences between WT, untreated Enpp1-deficient mice, and Enpp1-deficient mice treated with ERT 1118. Notably however, the bone-targeted ERT, administered at a dosage of 0.5 mg/kg body weight, was associated with an increased mineralization heterogeneity compared to WT and untreated Enpp1-deficient mice (Figure 4D). Notably, while the matrix mineralization was generally lower in the femur of the same animals, it was not decreased in *Enpp1*$^{asj/asj}$ mice compared to WT (Figure 4E).

Osteocyte lacunar mineralization as a unique phenomenon in ossicles of *Enpp1*$^{asj/asj}$ mice

Osteocytes, the most abundant cell type in bone, play a crucial role in regulating bone remodeling. To further elucidate the effects of Enpp1 deficiency on the osteocytic lacunar system, we analyzed the number, size, and morphology of osteocyte lacunae in the malleus of *Enpp1*$^{asj/asj}$ mice (Figure 5A). Both the osteocyte lacunar area and the total number of osteocyte lacunae did not differ between WT, untreated, and treated *Enpp1*$^{asj/asj}$ mice (Figure 5B and C). However, a significant reduction in the number of non-mineralized osteocyte lacunae in untreated *Enpp1*$^{asj/asj}$ mice compared to WT controls was found. Treatment with the soluble form of the enzyme did not normalize the number of non-mineralized osteocyte lacunae at any dosage tested (Figure 5D). In contrast, the bone-targeted form successfully normalized the number of non-mineralized lacunae at both 0.5 mg/kg and 1 mg/kg dosages. In untreated *Enpp1*$^{asj/asj}$ mice and in animals treated with the soluble ERT 1118, mineralized lacunae were apparent (Figure 5A and E). Lacunar mineralization was only prevented by bone-targeted ERT 2000 (Figure 5E). Since the mineralization of lacunae has not been previously described

Downloaded from https://academic.oup.com/jbmr/advance-article/doi/10.1093/jbmr/zjaf082/8160135 by ASBMR Member Access user on 04 August 2025

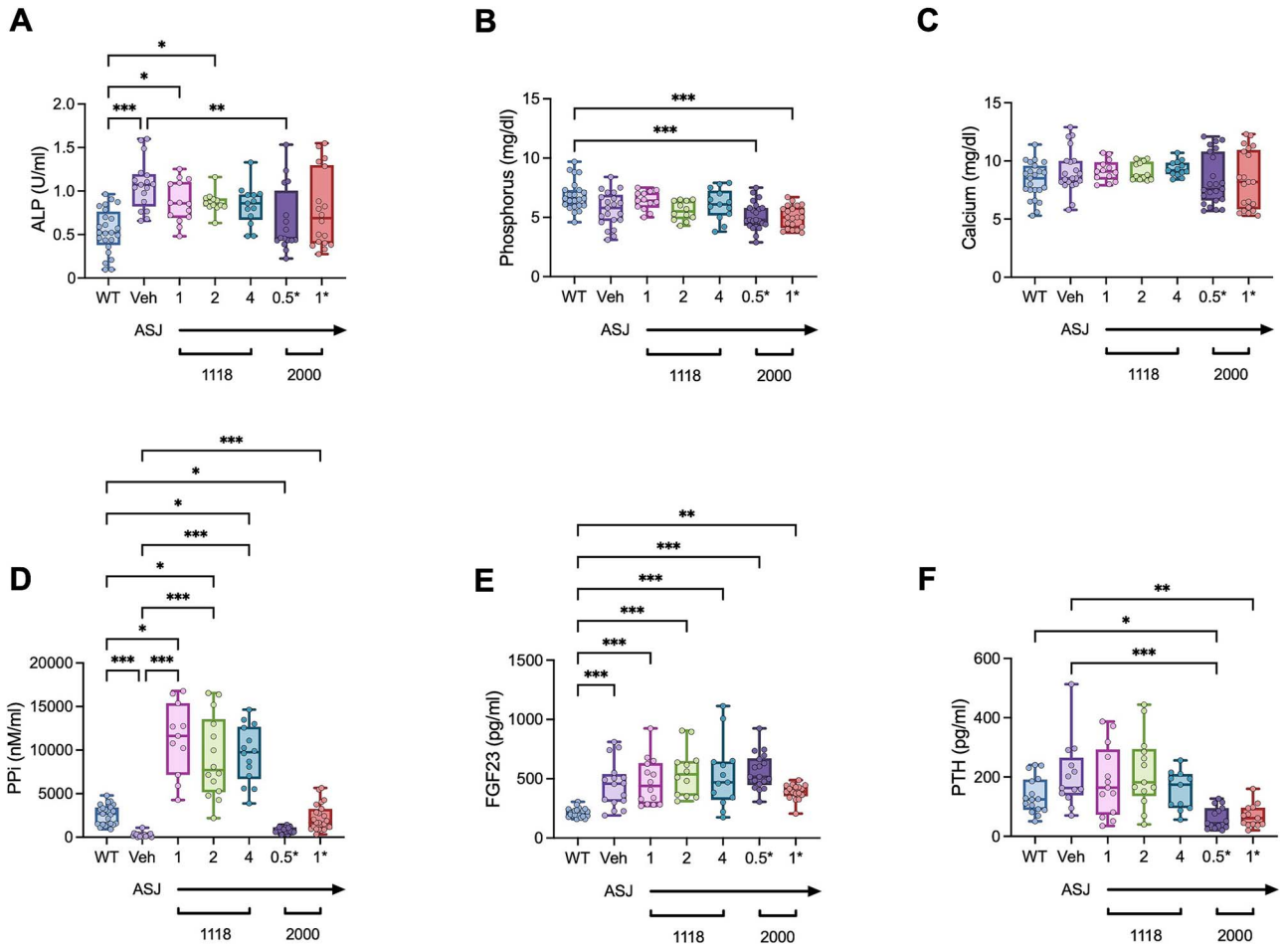

Figure 2. Blood plasma measurements in *Enpp1*$^{asj/asj}$ mice with different ERT formulations compared to untreated *Enpp1*$^{asj/asj}$ and WT mice. (A) Quantification of alkaline phosphatase (ALP), (B) phosphorus, (C) calcium, (D) PPi, (E) FGF23, and (F) PTH. Veh, vehicle (untreated). Statistical analysis was performed by ANOVA, with significance reported by Sidak's multiple comparisons tests comparing WT controls with untreated *Enpp1*$^{asj/asj}$ mice and WT or untreated *Enpp1*$^{asj/asj}$ mice with all treatment groups. $^{*}p < .05$, $^{**}p < .01$, $^{***}p < .001$. WT: $n = 24$, *Enpp1*$^{asj/asj}$+veh: $n = 17$, *Enpp1*$^{asj/asj}$+1 mg/kg 1118: $n = 14$, *Enpp1*$^{asj/as}$+2 mg/kg 1118: $n = 12$, *Enpp1*$^{asj/asj}$+4 mg/kg 1118: $n = 13$, *Enpp1*$^{asj/asj}$+0.5 mg/kg 2000: $n = 16$, *Enpp1*$^{asj/asj}$+1 mg/kg 2000: $n = 18$.

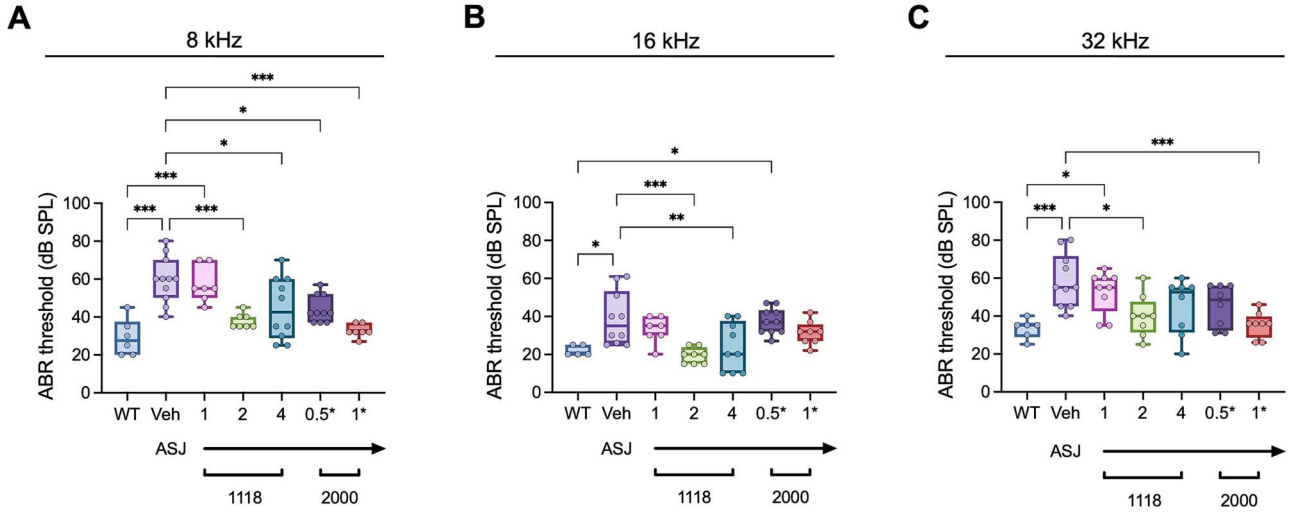

Figure 3. Functional hearing tests (ABR thresholds) in *Enpp1*$^{asj/asj}$ mice with different ERT formulations compared to untreated *Enpp1*$^{asj/asj}$ and WT mice. ABR measurements of 17-wk-old WT, untreated and treated *Enpp1*$^{asj/asj}$ mice at (A) 8, (B) 16, and (C) 32 kHz. Veh, vehicle (untreated). Statistical analysis was performed by ANOVA, with significance reported by Sidak's multiple comparisons tests comparing WT controls with untreated *Enpp1*$^{asj/asj}$ mice and WT or untreated *Enpp1*$^{asj/asj}$ mice with all treatment groups. $^{*}p < .05$, $^{**}p < .01$, $^{***}p < .001$. WT: $n = 5$, *Enpp1*$^{asj/asj}$+veh: $n = 10$, *Enpp1*$^{asj/asj}$+1 mg/kg 1118: $n = 7$, *Enpp1*$^{asj/asj}$+2 mg/kg 1118: $n = 7$, *Enpp1*$^{asj/asj}$+4 mg/kg 1118: $n = 8$, *Enpp1*$^{asj/asj}$+0.5 mg/kg 2000: $n = 8$, *Enpp1*$^{asj/asj}$+1 mg/kg 2000: $n = 7$.

Downloaded from https://academic.oup.com/jbmr/advance-article/doi/10.1093/jbmr/zjaf082/8160135 by ASBMR Member Access user on 04 August 2025

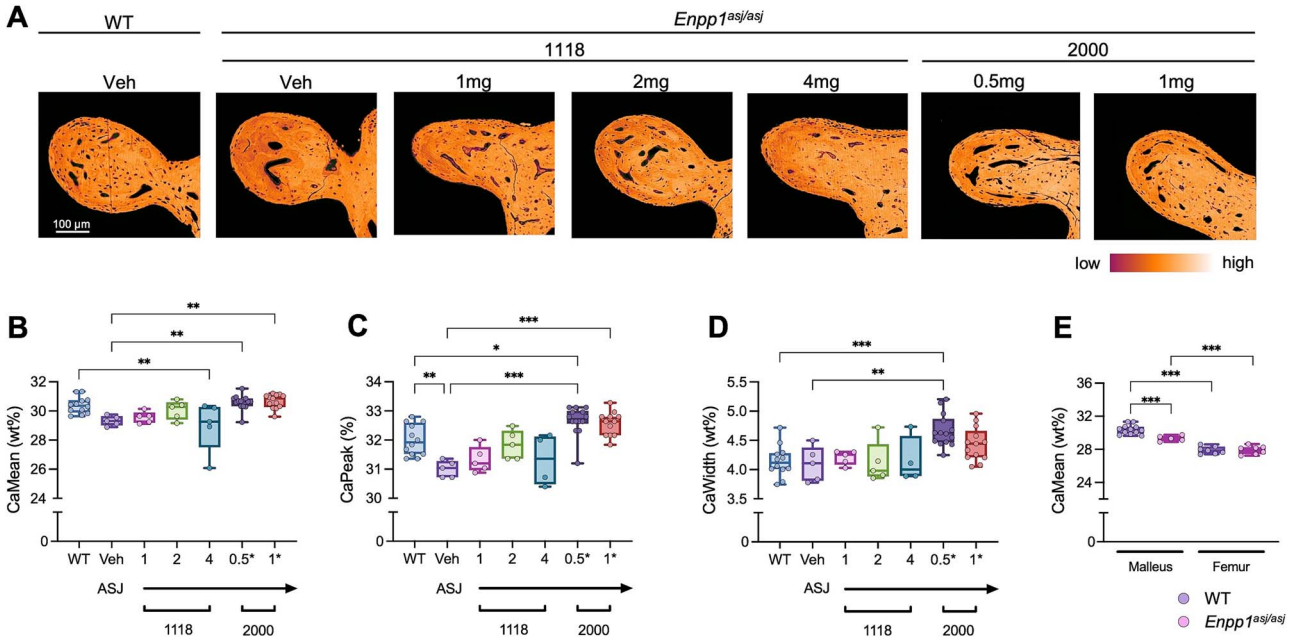

Figure 4. Mineralization properties in the different groups. (A) Representative quantitative backscattered electron images of the malleus from 17-wk-old WT, untreated and treated *Enpp1*$^{asj/asj}$ mice displaying the mineralization levels in pseudocolors (high and low mineralization are represented by bright and dark pixels, respectively). Scale bars: 100 μm. Quantitative analysis of (B) mean mineralization (CaMean), (C) peak mineralization properties (CaPeak) and (D) mineralization heterogeneity (CaWidth) of the malleus. Veh, vehicle (untreated). Statistical analysis in panels B-D was performed by ANOVA, with significance reported by Sidak's multiple comparisons tests comparing WT controls with untreated *Enpp1*$^{asj/asj}$ mice and WT or untreated *Enpp1*$^{asj/asj}$ mice with all treatment groups. WT: $n = 12$, *Enpp1*$^{asj/asj}$+veh: $n = 5$, *Enpp1*$^{asj/asj}$+1 mg/kg 1118: $n = 5$, *Enpp1*$^{asj/asj}$+2 mg/kg 1118: $n = 5$, *Enpp1*$^{asj/asj}$+4 mg/kg 1118: $n = 5$, *Enpp1*$^{asj/asj}$+0.5 mg/kg 2000: $n = 13$, *Enpp1*$^{asj/asj}$+1 mg/kg 2000: $n = 13$. (E) Comparison of CaMean between the malleus and femur of WT and Enpp1-deficient mice (ANOVA (Sidak), WT: malleus, $n = 12$, femur, $n = 7$, *Enpp1*$^{asj/asj}$: malleus, $n = 5$, femur, $n = 7$). $^{*}p < .05$, $^{**}p < .01$, $^{***}p < .001$.

in mice, we performed detailed analyses of their mineralization characteristics (Figure 5F). Comparison of the mean calcium content (CaMean) of mineralized osteocyte lacunae between untreated Enpp1-deficient mice and those treated with various doses of ERT 1118 indicated no differences (Figure 5G). Interestingly, however, the mineral within the osteocyte lacunae showed lower calcium content compared to the surrounding bone matrix, indicating a mechanism deviating from hypermineralization of human osteocyte lacunae (ie, micropetrosis). Using EDX, the atomic composition of mineralized lacunae in these mice was assessed. Similar to the observation determined by qBEI measurements, a difference of the calcium-to-phospahte ratio between untreated Enpp1-deficient mice and those treated with different dosages of ERT 1118 was not apparent (Figure 5H). Although presenting with a lower calcium content, the calcium-to-phosphate ratio of the mineralized osteocyte lacunae was similar to that of the adjacent bone, indicating that the intra-lacunar mineral is composed mainly of hydroxyapatite.

Discussion

Variants in the *ENPP1* gene cause different conditions depending on the patients' age, environmental factors, and mutation status, including GACI, ARHR2, EOOP, and OPLL, all of which are associated with hearing loss.[2,3,5,6] Although various hypotheses exist, the precise mechanisms underlying hearing impairment in these conditions are still not well understood. In this study, we therefore examined the auditory ossicles in Enpp1-deficient mice and found that mineralization defects and osteocyte dysfunction may contribute to the hearing loss observed, as evidenced by in-depth histomorphometric analyses and ABR testing, respectively. Interestingly, both bone-targeted and soluble ERT corrected hearing deficits in *Enpp1*$^{asj/asj}$ mice, while bone-targeted ERT also corrected bone abnormalities with a main effect on osteocyte lacunar properties. These findings offer a novel approach to treating hearing loss in patients with *ENPP1* variants.

Notably, the administration of bone-targeted ERT was associated with normalized hearing thresholds across tested frequencies. More specifically, while bone-targeted ERT at the higher dose of 1 mg/kg resulted in a partial correction of hearing loss at 16 kHz, a complete correction was observed at 8 and 32 kHz. Since this normalization was completely mirrored by trajectories of bone and osteocyte lacunar mineralization, the primary mechanism of hearing loss in Enpp1 deficiency may be related to dysfunction of the ossicular chain. While chronic inflammatory processes, such as chronic otitis media, have been associated with hearing loss both generally[18] and specifically in the context of *ENPP1* variants,[9,19] our findings reinforce that ossicular chain dysfunction plays a critical role in the auditory deficits observed. The ABR measurement at 32 kHz provides the most sensitive measurement given that mice demonstrate peak auditory sensitivity at frequencies between 15 and 20 kHz.[20] This frequency not only closely corresponds with the natural inclination of the mouse auditory system toward higher frequencies—distinct from human auditory capabilities—but is also critical for detecting subtle auditory changes not readily observable at lower frequencies. At 17 wk, mice are fully mature yet typically do not exhibit signs of age-related hearing loss, preferentially affecting higher frequencies initially.[21,22] Consequently, our setup allowed a

Downloaded from https://academic.oup.com/jbmr/advance-article/doi/10.1093/jbmr/zjaf082/8160135 by ASBMR Member Access user on 04 August 2025

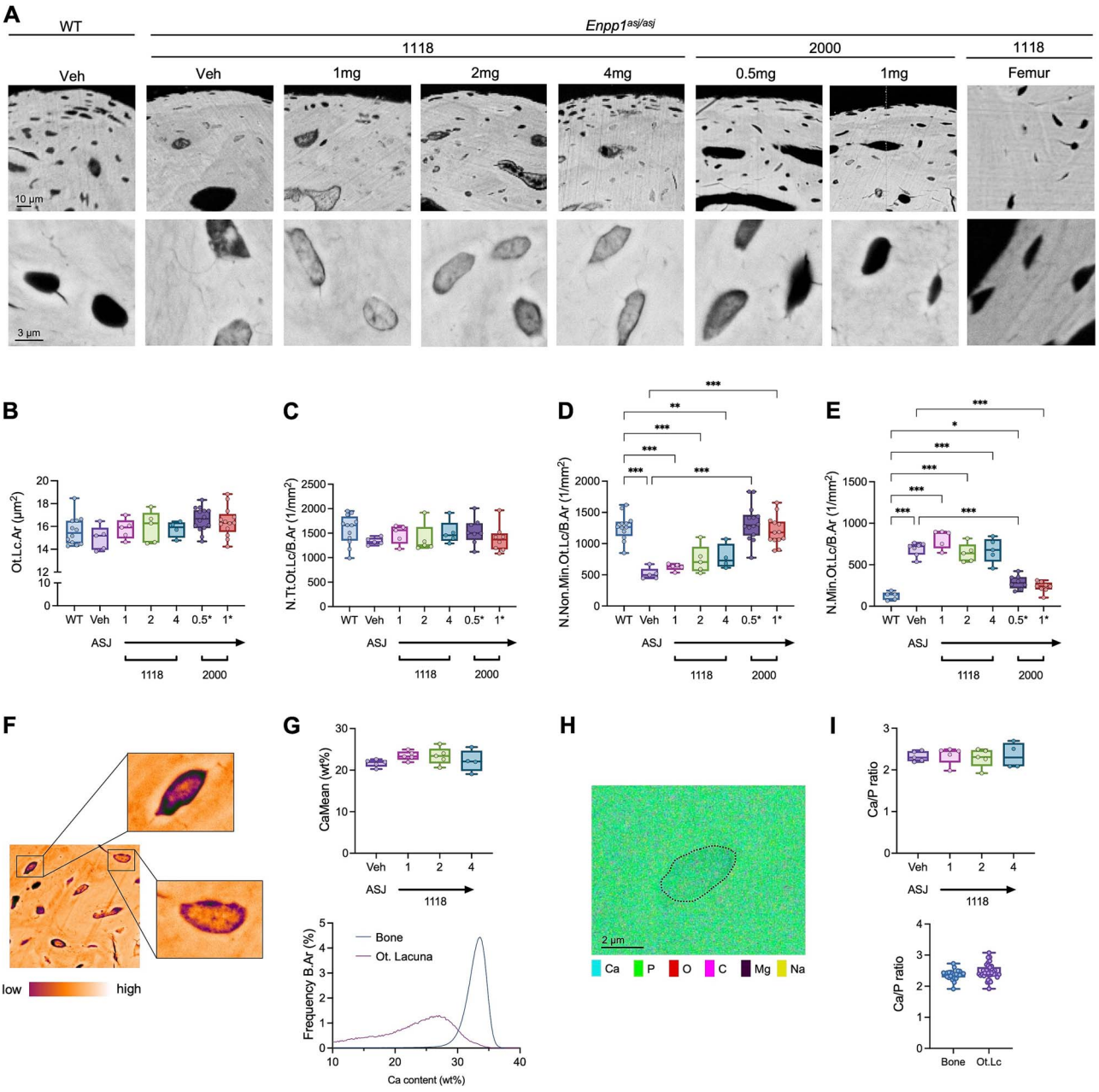

Figure 5. The osteocyte lacunar phenotype in *Enpp1*$^{asj/asj}$ mice with different ERT formulations compared to untreated *Enpp1*$^{asj/asj}$ and WT mice. (A) Representative quantitative backscattered electron images of the malleus from 17-wk-old WT, untreated and treated *Enpp1*$^{asj/asj}$ mice osteocyte lacunar morphology. Quantification of (B) osteocyte lacunar size, (C) density of osteocyte lacunae as well as (D) density and (E) proportion of mineralized lacunae. Statistical analysis in panels (B-E) was performed by ANOVA, with significance reported by Sidak's multiple comparisons tests comparing WT controls with untreated *Enpp1*$^{asj/asj}$ mice and WT or untreated *Enpp1*$^{asj/asj}$ mice with all treatment groups. WT: $n = 12$, *Enpp1*$^{asj/asj}$+veh: $n = 5$, *Enpp1*$^{asj/asj}$+1 mg/kg 1118: $n = 5$, *Enpp1*$^{asj/asj}$+2 mg/kg 1118: $n = 5$, *Enpp1*$^{asj/asj}$+4 mg/kg 1118: $n = 5$, *Enpp1*$^{asj/asj}$+0.5 mg/kg 2000: $n = 13$, *Enpp1*$^{asj/asj}$+1 mg/kg 2000: $n = 13$. (F) High-magnification qBEI images of mineralized lacunae in the malleus and (G) quantification of mean lacunar mineralization (CaMean, wt%) of Enpp1-deficient untreated and soluble ERT mice (upper panel). *Enpp1*$^{asj/asj}$+veh: $n = 5$, *Enpp1*$^{asj/asj}$+1 mg/kg 1118: $n = 5$, *Enpp1*$^{asj/asj}$+2 mg/kg 1118: $n = 5$, *Enpp1*$^{asj/asj}$+4 mg/kg 1118: $n = 4$. Pooled BMD distribution of osteocyte lacunae of all analyzed groups indicate a low and inhomogeneous mineralization pattern of mineralized osteocyte lacunae compared to the bone matrix (lower panel). (H) Representative layered EDX image of a mineralized osteocyte lacuna (encircled by a dotted line) and adjacent bone in a malleus of an Enpp1-deficient mouse treated with 1 mg/kg ERT 1118. The pseudo-colored image represents the weight percentage distribution of calcium (Ca), phosphate (P), oxide (O), carbon (C), magnesia (Mg), and sodium (Na) and indicates a similar proportion in the matrix and lacuna. (I) Quantification of lacunar mineral composition (Ca/P ratio) by EDX in the malleus of Enpp1-deficient untreated and soluble ERT mice (upper panel) and pooled comparison of all lacunae with the surrounding bone matrix. Veh, vehicle (untreated). *Enpp1*$^{asj/asj}$+veh: $n = 5$, *Enpp1*$^{asj/asj}$+1 mg/kg 1118: $n = 5$, *Enpp1*$^{asj/asj}$+2 mg/kg 1118: $n = 5$, *Enpp1*$^{asj/asj}$+4 mg/kg 1118: $n = 4$. $^{*}p < .05$, $^{**}p < .01$, $^{***}p < .001$.

precise assessment of hearing function before the onset of age-related decline.

We have previously demonstrated in another mouse model of poor matrix mineralization, that is, the *Hyp* model of X-linked hypophosphatemia, that conductive hearing is accompanied by hypomineralization of the auditory ossicles.[10] Of note, we have also previously shown that dietary vitamin D supplementation was associated with improved

Downloaded from https://academic.oup.com/jbmr/advance-article/doi/10.1093/jbmr/zjaf082/8160135 by ASBMR Member Access user on 04 August 2025

matrix mineralization of auditory ossicles in Vdr knock out ($Vdr^{-/-}$) mice.[15] However, further therapeutic aspects remained unanswered in previous work, in particular the question of whether an improvement in the mineralization of the auditory ossicles is accompanied by improved hearing function. Here we could show in the $Enpp1^{asj/asj}$ model that an improvement of hearing function by bone-targeted ERT was closely related to an improvement of matrix mineralization of the malleus measured by qBEI. Based on our results, the efficacy of this treatment concept in patients with genetic bone diseases with poor matrix mineralization and hearing loss should be further investigated. Early treatment, as in this model after weaning, is presumably crucial, as the ossification and mineralization of ossicles is completed very early in both humans and mice.[10,23]

The bone-targeted form of ERT also effectively normalized the number of non-mineralized osteocyte lacunae at both applied doses, demonstrating a strong potential to counter the cellular anomalies associated with Enpp1 deficiency. In particular, this form of ERT also significantly reduced the number of mineralized osteocyte lacunae, emphasizing its targeted action on key bone mineralization processes and further highlighting the therapeutic potential of targeting osteocytic pathways. In humans, the phenomenon of osteocyte lacunar mineralization is called micropetrosis. Micropetrosis has been associated with aging and immobilization and has been found to be indicative of osteocyte apoptosis.[24–27] In human auditory ossicles, the near absence of bone resorption by osteoclasts has been associated with an early appearance of mineralized osteocyte lacunae.[23] Importantly, the mineralization of the osteocyte lacunae in the Enpp1-deficient mice studied here clearly differs from the phenomenon of human micropetrosis since the intra-lacunar mineral exhibited a lower calcium content than the surrounding bone matrix, while in human micropetrosis it tends to be more highly mineralized than the adjacent bone.[27] Another difference is the absence of mineralized pearl (ie, spherite) formation in murine Enpp1 deficiency compared to human micropetrosis.[27] Of further interest is that osteocyte lacunar mineralization was observed exclusively in the ossicles but not in other bones, such as the femur. Since osteocytes represent terminally differentiated osteoblasts, one cause for the observed mineralized osteocyte lacunae may be that type II collagen-producing hypermineralizing osteoblast subtypes (termed auditory osteoblasts), previously identified in murine ossicles,[28] are more susceptible to mineralization when differentiated into osteocytes under pathological conditions, such as in Enpp1 deficiency. Here, the formation and dissolution of mineralized osteocyte lacunae was characterized for the first time in mice. Interestingly, osteocyte lacunae in Enpp1-deficient mice presented with smaller osteocyte lacunae in almost all analyzed weight-bearing bones.[2,4,11,12] Although this was not associated with signs of osteocyte lacunar mineralization at other skeletal sites in most studies, one study indicated mineralization of osteocyte lacunae also in long bones of Enpp1-deficient mice.[29]

The restoration of both structural, cellular, and functional parameters reflects the potential of bone-targeted ERT for clinical application. Patients with GACI often exhibit a range of hearing impairments, from mild to moderate conductive hearing loss, and less commonly, sensorineural hearing loss.[19] Our findings suggest an increased risk for hearing loss and thus underscore the need for ongoing audiologic and otolaryngologic evaluations in these patients. Early detection and intervention are critical, as they can significantly mitigate language and cognitive impairments in affected individuals.[30] The promising results of bone-targeted ERT in reversing hearing loss and bone anomalies provide a solid foundation for integrating this therapy into treatment strategies for patients with *ENPP1*-related disorders. Future research should focus on long-term outcomes, optimizing dosing regimens, and potentially expanding these findings to human clinical trials to substantiate and refine the use of ERT in clinical settings.

Our study has several limitations. A key limitation of our study is the inability to definitively distinguish between conductive and sensorineural hearing loss in Enpp1-deficient mice using the applied auditory assessments. While ABR testing provides valuable insights into hearing thresholds, it does not differentiate between conductive and sensorineural components. Additional methods such as otoacoustic emissions or tympanometry would have been necessary to confirm the presence of conductive hearing loss. Furthermore, histological analysis of the cochlea, spiral ganglion neurons, and middle ear structures would have been necessary to determine whether Enpp1 deficiency contributes to inner ear pathology, potentially leading to a mixed hearing loss phenotype. In addition, we did not examine soft tissue structures of the middle ear (eg, epithelium), which play an important role in the pathogenesis of conductive hearing loss, for example, in the context of otitis media. However, the fact that the hearing loss in people with GACI is conductive in 80% of cases,[19] together with the profound impairment of ossicular bone mineralization in Enpp1-deficient mice described here, suggests that the hearing loss is attributable largely to the middle ear. A further limitation of our work is that we focused on male mice in all our experiments. However, although Enpp1 is not inherited on the sex chromosomes, the overall skeletal status may differ between male and female mice, making a combined analysis of both sexes impractical. To reduce the number of animals required in this animal experiment, we therefore focused on the analysis of male animals, which aligns with the 3R principles. Another limitation is that our study did not explore potential adverse events associated with ERT. Finally, because our study was conducted in mice, its generalizability to humans is limited. However, clinical trials are currently underway to evaluate the response to a newly developed ERT. These studies will monitor the effects on patients' hearing and either confirm or challenge our findings.

Taken together, our results show an improvement of auditory function in Enpp1-deficient mice by the application of ERT, together with the correction of a distinct phenotype in the auditory ossicles in the form of a combination of low mineralization of the bone matrix and mineralized osteocyte lacunae. These results suggest the potential benefit of correcting bone mineralization to prevent hearing loss in Enpp1 deficiency.

Acknowledgments

The authors would like to thank Andrea Thieke, Olga Winter, and Annette Jung for their excellent technical assistance.

Author contributions

Ana Ocokoljic (Methodology, Formal analysis, Validation, Investigation, Data curation, Writing—original draft, Visualization [equal]),

Downloaded from https://academic.oup.com/jbmr/advance-article/doi/10.1093/jbmr/zjaf082/8160135 by ASBMR Member Access user on 04 August 2025

Shivani Srivastava (Conceptualization, Validation, Investigation, Resources, Writing—review & editing [equal]), Simon von Kroge (Investigation, Writing—review & editing), Paul R. Stabach (Investigation, Writing—review & editing), Björn Busse (Methodology, Investigation, Writing—review & editing), Keith Weise (Investigation, Writing—review & editing), Ralf Oheim (Conceptualization, Investigation, Writing—review & editing), Tim Rolvien (Conceptualization, Methodology, Resources, Writing—original draft, Writing—review & editing, Visualization, Supervision, Project administration [equal]), and Demetrios T. Braddock (Conceptualization, Methodology, Resources, Writing—review & editing, Visualization, Supervision, Project administration [equal])

Ana Ocokoljic and Shivani Srivastava contributed equally to this work. Tim Rolvien and Demetrios T. Braddock jointly supervised this work.

Funding

This research received funding from UKE-Stiftung to T.R., from the German Research Foundation (DFG) to T.R. and R.O. within the Clinical Research Unit *ProBone* under the grant numbers RO 5925/5-1 and OH324/2-1, respectively, and from the National Institutes of Health (R01AR080416) and Inozyme Pharma to D.T.B.

Conflicts of interest

A.O., S.S., S.v.K., B.B., K.W., and T.R. declare no conflict of interest. R.O. has served as a speaker and advisory board member for Kyowa Kirin, Inozyme, Ipsen, Pharmacosmos, Mereo, and UCB and has received institutional research grants from Kyowa Kirin, UCB, and Inozyme. D.T.B. and P.R.S. are inventors on patents owned by Yale University for therapeutics treating ENPP1 deficiency. D.T.B. is an equity holder and receives research and consulting support from Inozyme Pharma.

Data availability

The data that support the findings of this study are available from the corresponding author upon reasonable request.

Study approval

Animal studies were approved by the Animal Care and Use Committee of Yale University and adhered to the U.S. National Institutes of Health guidelines for the care and use of laboratory animals.

References

1. Harmey D, Hessle L, Narisawa S, Johnson KA, Terkeltaub R, Millan JL. Concerted regulation of inorganic pyrophosphate and osteopontin by akp2, enpp1, and ank: an integrated model of the pathogenesis of mineralization disorders. *Am J Pathol*. 2004;164(4):1199-1209. https://doi.org/10.1016/S0002-9440(10)63208-7
2. Ferreira CR, Kavanagh D, Oheim R, et al. Response of the ENPP1-deficient skeletal phenotype to oral phosphate supplementation and/or enzyme replacement therapy: comparative studies in humans and mice. *J Bone Miner Res*. 2021;36(5):942-955. https://doi.org/10.1002/jbmr.4254
3. Rutsch F, Böyer P, Nitschke Y, et al. Hypophosphatemia, hyperphosphaturia, and bisphosphonate treatment are associated with survival beyond infancy in generalized arterial calcification of infancy. *Circ Cardiovasc Genet*. 2008;1(2):133-140. https://doi.org/10.1161/CIRCGENETICS.108.797704
4. Zimmerman K, Liu X, von Kroge S, et al. Catalysis-independent ENPP1 protein signaling regulates mammalian bone mass. *J Bone Miner Res*. 2022;37(9):1733-1749. https://doi.org/10.1002/jbmr.4640
5. Levy-Litan V, Hershkovitz E, Avizov L, et al. Autosomal-recessive hypophosphatemic rickets is associated with an inactivation mutation in the ENPP1 gene. *Am J Hum Genet*. 2010;86(2):273-278. https://doi.org/10.1016/j.ajhg.2010.01.010
6. Lorenz-Depiereux B, Schnabel D, Tiosano D, Häusler G, Strom TM. Loss-of-function ENPP1 mutations cause both generalized arterial calcification of infancy and autosomal-recessive hypophosphatemic rickets. *Am J Hum Genet*. 2010;86(2):267-272. https://doi.org/10.1016/j.ajhg.2010.01.006
7. Kato H, Ansh AJ, Lester ER, et al. Identification of ENPP1 haploinsufficiency in patients with diffuse idiopathic skeletal hyperostosis and early-onset osteoporosis. *J Bone Miner Res*. 2022;37(6):1125-1135. https://doi.org/10.1002/jbmr.4550
8. Kato H, Braddock DT, Ito N. Genetics of diffuse idiopathic skeletal hyperostosis and ossification of the spinal ligaments. *Curr Osteoporos Rep*. 2023;21(5):552-566. https://doi.org/10.1007/s11914-023-00814-6
9. Tian C, Harris BS, Johnson KR. Ectopic mineralization and conductive hearing loss in Enpp1asj mutant mice, a new model for otitis media and tympanosclerosis. *PLoS One*. 2016;11(12):e0168159. https://doi.org/10.1371/journal.pone.0168159
10. Delsmann MM, Seist R, Stürznickel J, et al. Conductive hearing loss in the Hyp mouse model of X-linked hypophosphatemia is accompanied by hypomineralization of the auditory ossicles. *J Bone Miner Res*. 2021;36(12):2317-2328. https://doi.org/10.1002/jbmr.4443
11. Oheim R, Zimmerman K, Maulding ND, et al. Human heterozygous ENPP1 deficiency is associated with early onset osteoporosis, a phenotype recapitulated in a mouse model of Enpp1 deficiency. *J Bone Miner Res*. 2020;35(3):528-539. https://doi.org/10.1002/jbmr.3911
12. Li Q, Guo H, Chou DW, Berndt A, Sundberg JP, Uitto J. Mutant Enpp1asj mice as a model for generalized arterial calcification of infancy. *Dis Model Mech*. 2013;6(5):1227-1235. https://doi.org/10.1242/dmm.012765
13. Albright RA, Stabach P, Cao W, et al. ENPP1-Fc prevents mortality and vascular calcifications in rodent model of generalized arterial calcification of infancy. *Nat Commun*. 2015;6(1):10006. https://doi.org/10.1038/ncomms10006
14. Stabach PR, Zimmerman K, Adame A, et al. Improving the pharmacodynamics and in vivo activity of ENPP1-Fc through protein and glycosylation engineering. *Clin Transl Sci*. 2021;14(1):362-372. https://doi.org/10.1111/cts.12887
15. Delsmann MM, Peichl J, Yorgan TA, et al. Prevention of hypomineralization in auditory ossicles of vitamin D receptor (Vdr) deficient mice. *Front Endocrinol (Lausanne)*. 2022;13:901265. https://doi.org/10.3389/fendo.2022.901265
16. Alimy AR, Thiessen ML, Strahl A, et al. Sex-specific Association of Clinical Parameters and Components of femoral bone quality in patients undergoing total hip arthroplasty. *Calcif Tissue Int*. 2024;115(5):570-580. https://doi.org/10.1007/s00223-024-01286-1
17. Danyukova T, Alimy AR, Velho RV, et al. Mice heterozygous for an osteogenesis imperfecta-linked MBTPS2 variant display a compromised subchondral osteocyte lacunocanalicular network associated with abnormal articular cartilage. *Bone*. 2023;177:116927. https://doi.org/10.1016/j.bone.2023.116927
18. Delsmann MM, Bonik P, Ocokoljic A, et al. Cholesteatoma severely impacts the integrity and bone material quality of the incus. *Calcif Tissue Int*. 2023;113(6):609-617. https://doi.org/10.1007/s00223-023-01144-6
19. Theng EH, Brewer CC, Oheim R, et al. Characterization of hearing-impairment in generalized arterial calcification of infancy (GACI). *Orphanet J Rare Dis*. 2022;17(1):273. https://doi.org/10.1186/s13023-022-02410-w
20. Zheng QY, Johnson KR, Erway LC. Assessment of hearing in 80 inbred strains of mice by ABR threshold analyses. *Hear*

Downloaded from https://academic.oup.com/jbmr/advance-article/doi/10.1093/jbmr/zjaf082/8160135 by ASBMR Member Access user on 04 August 2025

Res. 1999;130(1-2):94-107. https://doi.org/10.1016/S0378-5955(99)00003-9
21. Li HS, Borg E. Age-related loss of auditory sensitivity in two mouse genotypes. *Acta Otolaryngol*. 1991;111(4):827-834. https://doi.org/10.3109/00016489109138418
22. Zeng L, Zhou W, Bing D, Xie L, Wang X, Zhang G. Protocol for assessing auditory brainstem response in mice using a four-channel recording system. *STAR Protoc*. 2022;3(2):101251. https://doi.org/10.1016/j.xpro.2022.101251
23. Rolvien T, Schmidt FN, Milovanovic P, et al. Early bone tissue aging in human auditory ossicles is accompanied by excessive hypermineralization, osteocyte death and micropetrosis. *Sci Rep*. 2018;8(1):1920. https://doi.org/10.1038/s41598-018-19803-2
24. Rolvien T, Milovanovic P, Schmidt FN, et al. Long-term immobilization in elderly females causes a specific pattern of cortical bone and osteocyte deterioration different from postmenopausal osteoporosis. *J Bone Miner Res*. 2020;35(7):1343-1351. https://doi.org/10.1002/jbmr.3970
25. Milovanovic P, Busse B. Phenomenon of osteocyte lacunar mineralization: indicator of former osteocyte death and a novel marker of impaired bone quality? *Endocr Connect*. 2020;9(4):R70-r80. https://doi.org/10.1530/EC-19-0531
26. Milovanovic P, Busse B. Micropetrosis: osteocyte lacunar mineralization in aging and disease. *Curr Osteoporos Rep*. 2023;21(6):750-757. https://doi.org/10.1007/s11914-023-00832-4
27. Milovanovic P, Zimmermann EA, Vom Scheidt A, et al. The formation of calcified Nanospherites during Micropetrosis represents a unique mineralization mechanism in aged human bone. *Small*. 2017;13(3). https://doi.org/10.1002/smll.201602215
28. Kuroda Y, Kawaai K, Hatano N, et al. Hypermineralization of hearing-related bones by a specific osteoblast subtype. *J Bone Miner Res*. 2021;36(8):1535-1547. https://doi.org/10.1002/jbmr.4320
29. Hajjawi MO, MacRae VE, Huesa C, et al. Mineralisation of collagen rich soft tissues and osteocyte lacunae in Enpp1(-/-) mice. *Bone*. 2014;69:139-147. https://doi.org/10.1016/j.bone.2014.09.016
30. Park SY, Ho SH, Hong YJ, et al. The effect of hearing loss on cognitive function in subjective cognitive decline. *Dement Geriatr Cogn Disord*. 2022;51(4):348-356. https://doi.org/10.1159/000526230

Downloaded from https://academic.oup.com/jbmr/advance-article/doi/10.1093/jbmr/zjaf082/8160135 by ASBMR Member Access user on 04 August 2025

© The Author(s) 2025. Published by Oxford University Press on behalf of the American Society for Bone and Mineral Research. All rights reserved. For commercial re-use, please contact reprints@oup.com for reprints and translation rights for reprints. All other permissions can be obtained through our RightsLink service via the Permissions link on the article page on our site—for further information please contact journals.permissions@oup.com.
Journal of Bone and Mineral Research, 2025, 00, 1–10
https://doi.org/10.1093/jbmr/zjaf082
Research Article